Environmental Science and Pollution Research (2022) 29:82390–82410
https://doi.org/10.1007/s11356-022-21505-2

RESEARCH ARTICLE

Energy, exergy, environmental impact, and economic analyses of evacuated tube compound parabolic concentrator–powered solar thermal domestic water heating system

Dinesh Kumar Sharma[1,2] · Dilip Sharma[2] · Ahmed Hamza H. Ali[3]

Received: 9 December 2021 / Accepted: 12 June 2022 / Published online: 25 June 2022

Abstract

In the reported study, a dynamic analytical model is developed to propose the energy, exergy, environmental impact, and economic analyses of the water heating system at Jaipur (India) with an evacuated tube compound parabolic concentrator field of a total area of 81 m^2. Consequently, the model is used to perform parametric studies to report the effect of operating and meteorological parameters on the productivity and performance of the system. Moreover, the system's performance, environmental impact, and economic aspects have been investigated and compared under different meteorological conditions at four different Rajasthan (India) locations using TMY2 weather data files. Results clarified that Jodhpur receives the highest solar radiation intensity from these four locations. The model results were validated with the experimental data, and a good agreement has prevailed. Consequently, the results indicate the highest annual energy and exergy gain for Jodhpur with 79.72 MWh and 9.311 MWh, respectively, followed by Jaisalmer, Barmer, and Jaipur. The economic analysis results clarified that the simple payback period ranged from 4.5 to 4.75 years and the discounted payback period ranged from 6.6 to 7 years based on a 6% discount rate. At the same time, the levelized cost of heating for the given system is around 0.023 $/kWh which is very economical closest to that of CNG as a fuel which costs around 0.059 $/kWh. The internal rate of return is reported to be 16.76, 16.82, 16.77, and 16.75% for Barmer, Jodhpur, Jaipur, and Jaisalmer, respectively, and savings of 74.4, 78.1, 75.4, and 73.8 tonnes of CO_2 emission to the environment.

Keywords Energy · Exergy · Environmental impact · Economic · Evacuated tube · Compound parabolic concentrator

Nomenclature

CC	Construction/installation cost
CF	Cash flows
CI	Cash inflows
CNG	Compressed natural gas
CPC	Compound parabolic concentrator
CV	Calorific value
DPBP	Discounted payback period
ETC	Evacuated tube collector
ET-CPC	Evacuated tube with compound parabolic concentrator
FPC	Flat-plate collector
IRR	Internal rate of return
LCOH	Levelized cost of heating
LPG	Liquefied petroleum gas
PCM	Phase change material
PTC	Parabolic trough collector
RTD	Resistance temperature detector
SDWH	Solar domestic water heating
SPBP	Simple payback period
SPV	Solar photovoltaic
STC	Solar thermal collector
TES	Thermal energy storage
TLCC	Total life cycle cost

Responsible Editor: Eyup Dogan

✉ Dinesh Kumar Sharma
dinesh.sharma@skit.ac.in

Dilip Sharma
sharmadmnit@gmail.com

Ahmed Hamza H. Ali
ah-hamza@aun.edu.eg

[1] Department of Mechanical Engineering, Swami Keshvanand Institute of Technology, Management and Gramothan, 302017 Jaipur, India

[2] Department of Mechanical Engineering, Malaviya National Institute of Technology, Jaipur 302017, India

[3] Department of Mechanical Engineering, Assiut University, Assiut 71516, Egypt

Symbols and notations

A	Area (m^2)
C_f	Specific heat (J/kg K)
D	Tube diameter (m)
dt	Time difference (s)
Ex	Exergy (W/m^2)
f	Friction factor
F_R	Heat removal factor
h	Convective heat transfer coefficient ($W/m^2.K$)
I_T	Total solar radiation (W/m^2)
K_{eff}	Effective constant
L	Length (m)
$\dot{m}_f$	Mass flow rate (kg/s)
n	Number of measurements
P	Pressure (kPa)
Q_{useful}	Useful heat gain (kWh)
R	Tube radius (m)
Re	Reynolds number
s	Specific entropy (kJ/kg K)
SD	Standard deviation
T	Temperature (°C)
V	Fluid velocity (m/s)
U_L	Overall heat transfer coefficient ($W/m^2.K$)
U_{tpa}	Overall heat transfer coefficient top to ambient (W/m^2 .K)
X_m	Measured values
Z_{env}	Cost of penalty ($)

Greek letter

α	Absorptivity
ρ	Density
η	Efficiency
λ	Emission conversion factor
Ψ	Exergetic efficiency
μ	Kinematic viscosity
τ	Transmissivity

Subscript/superscript

abs	Absorption
amb	Ambient
c	Collector
cond	Conduction
eff	Effective
f	Fluid
in	Inlet
m	Mean
n	Number of collector in-series
out	Outlet
opt	Optical
r	Receiver

Introduction

The primary driver of shifting toward renewable energy resources is climate change, as the world energy demands are being met mainly by conventional energy resources, which are responsible for contributing harmful pollutants to the environment (Panahi et al. 2019). Renewable energy resources such as solar energy have been proven to meet the energy demand without leaving a carbon footprint. Nevertheless, these technologies often have many challenges in providing a stable and reliable energy supply (Boukelia et al. 2021). Solar thermal collectors (STCs) and solar photovoltaic panels (SPVs) are promising technologies harnessing solar energy and using it for cooling, heating, and power. Some of the popular solar thermal conversion technologies are flat-plate collectors (FPCs), compound parabolic concentrators (CPCs), evacuated tube collectors (ETCs), and parabolic trough collectors (PTCs). Recent innovations and technological advancements such as evacuated tubes integrated with CPC (ET-CPC), evacuated tubes integrated with PTC, and many others have excellent productivity and reduced heat losses to the environment. ET-CPCs are most preferred for applications in the medium operating temperature range (up to 150 °C) of a stationary type of STCs. Also, these provide excellent productivity through the utilization of both diffused and direct radiations with thermal efficiencies ranging from 35 to 55%.

Domestic/community water heating is an essential application that is energy-intensive, and the use of conventional resources such as kerosene, natural gas, wood, coal, and electricity is quite expensive and emits harmful emissions. Earlier, FPC was the primary choice for domestic water heating applications, but technological advancements in STCs such as ETCs and ET-CPCs can also be seen as more efficient and better options referring to the literature. In one study, Sokhansefat et al. (2018) compared the FPC and ETC solar collectors in cold climatic conditions based on thermoeconomic and environmental impact analyses. It was reported that the performance of the ETC system is 41% more efficient than the FPC-based system, and the yearly practical heat gain of ETC is up to 30% more as compared to FPC. In another study, Hazami et al. (2013) reported year-round energy performance monitoring results of a new solar domestic water heating (SDWH) system powered by ETCs. It was concluded that ETCs generated about 9% more energy than the FPC under the same climatic condition. Kabeel et al. (2020) discussed the thermal performance of modified ETC, which was integrated with low-cost concentrators, and graphite nanomaterial was used as hybrid storage materials in the mass concentrations of 2 to 5%. The thermal efficiency of the modified design was recorded to be 72.1%.

Despite the excellent performance of ETC as a solar heat conversion technology, the low intercept area was a significant challenge that allowed large amounts of untapped solar radiation to pass through. In an attempt to fulfill this gap, Ma et al. (2010) reported that CPC reflectors at the backside of the ETC tubes are helpful to increase the collector efficiency by improving the overall aperture area. After that, Pei et al. (2012) analyzed the ET-CPCs and concluded that the CPC reflectors are helpful to improve the thermal performance of the ETCs in high-temperature ranges. In another study, Jiang et al. (2015) analyzed the performance of the ET-CPCs and reported an instantaneous efficiency of 50% using mineral oils as a working fluid while operating at a temperature of 200 °C. Furthermore, Mills et al. (1986) analyzed the effect of the acceptance angle of CPC on the performance of the evacuated tubes. It is concluded that the acceptance angle is less decisive, but the aperture area is. The performance of the ET-CPC is reported to have a negligible effect on the selection of orientation from North-South or East-West. The selection of the CPC reflector material is also reported and informed that the use of polished stainless steel is better in terms of cost-effectiveness, durability, and maintenance as compared to other mirror materials. Geete et al. (2019) fabricated compound parabolic solar collectors with evacuated tubes and analyzed the system's thermal performance. The instantaneous energy efficiency during the experiments was 69.87%, significantly higher than both FPCs and ETCs.

Previously, Mishra et al. (2017) compared the thermal performance of ETC and ET-CPC based on energy and exergy analyses. It was reported that an additional 27.28% extra gain in energy was recorded with ET-CPC compared to ETC, while a 20.9% gain was reported in exergy. In another study, Kerme et al. (2017) presented an energy and exergy analyses of a solar-powered vapor absorption system powered by ET-CPC. From the analysis, the primary source of exergy loss is the solar collector, as about 71.9% of the total exergy loss of 84% was through the solar collector only. Furthermore, Chopra et al. (2021) reported an energy, exergy, environmental, and economic analyses of a phase change material (PCM)–embedded ETC-powered solar water heating system. A significant improvement was shown in energy, exergy, and CO_2 mitigation using ETC with PCM compared to without PCM. The results claimed a rise of 36–44% in energy efficiency, whereas a rise of 28–35% was observed in exergy efficiency using PCM filled in annular space between absorber and tube of ETC. In addition to this, nanofluids are also recommended to improve further solar collectors' thermal performance (Faizal et al. 2015).

For various operating scenarios, Bellos et al. (2017) reported energy, exergy, environmental impact, and economic analyses for a solar-assisted refrigeration system. The dynamic energy and exergy analyses were conducted based on the daily average solar data (Arslan and Kilic 2021). Thus, a suitable way was offered on the environmental tax, including the value-added tax discount or a new carbon tax ranging between 5 and 18%. Battisti and Corrado (2005) applied environmental analysis and optimization to the water storage coupled solar thermal collector. SimaPro software program was used to obtain environmental indicators. It was found that the reduction of the impacts could be up to 40%, and the environmental payback times were 5–19 months. Evacuated tube collectors fed heat to the generator of the vapor absorption chiller. The electricity savings were 53.98%, the internal rate of return (IRR) 6.6%, and the payback period close to 14 years.

Thus, it can be concluded that ET-CPCs are pretty efficient at elevated temperatures up to 200 °C and have no need for a solar tracking mechanism, which makes them a preferred choice over FPC. Simultaneously, a significant advantage of using ET-CPCs is using both diffuse and direct solar radiation. The thermodynamic performance of ET-CPCs-based solar water heating systems has been measured through energy and exergy analyses. Energy analysis is conservative as per the first law of thermodynamics which typically involves energy efficiency and gain. On the other hand, exergy analysis helps determine the energy transactions based on quality. Exergy analysis denotes the maximum theoretical work obtained in given environmental conditions. Therefore, it is essential to consider the quantity and quality of the energy used for practical energy usage (Saidur et al. 2010; Cengel et al. 2019). Hence, a thermodynamic system can be better assessed with the help of an exergy method (Caliskan 2017). Expressing the actual efficiency makes the exergy a powerful tool in sectoral energy analysis and engineering design (Rosen and Dincer 1997). Also, exergy analysis helps determine the system's sustainability (Moran and Shapiro 1993). An overall analysis of the system is incomplete without understanding its monetary transactions and environmental impact during its entire useful life (Dincer and Rosen 2007; Meyer et al. 2009). It should be pointed out that economic analysis is indirectly affected by environmental impact and energy analysis results (Tsatsaronis and Morosuk 2012). Beyond exergy analysis, several other indicators such as enviroeconomic, exergoeconomic, exergoenvironmental, and life cycle cost analysis depict a clear understanding of the sustainability of the renewable energy solutions over the conventional ones (Rosen 2018). Furthermore, previous studies show that the exergo-environmental performance of a renewable energy system can be boosted by minimizing the rate of exergy dissipation (Aghbashlo et al. 2019).

In the present work, an analytical model is developed to carry out energy, exergy, environmental impact, and economic analyses of an 81m^2 ET-CPC-powered solar water heating system equipped with thermal energy storage. A parametric study is also performed to report the effect of

mass flow rate, solar radiation intensity and ambient temperature on productivity and efficiency of reported installation at various fluid inlet temperatures. This work's novelty lies in the inclusion of sensible thermal energy storage being energized with the help of the most efficient and state-of-the-art design from stationary STCs referred to as ET-CPC. Simultaneously, the need for a dynamic analytical model cannot be denied to show the impact of multiple real-time input parameters on the thermodynamic performance of the integrated ET-CPC solar field with sensible thermal energy storage. Furthermore, it was identified that overall analysis of ET-CPC-based applications is less reported in the literature, and thus, sufficient data is not available which can be otherwise helpful to promote its use. Thus, the thermodynamic performance of the SDWH system with its environmental impact and economic aspects has been investigated and compared under meteorological conditions in four different locations of Rajasthan (India) using TMY2 weather data files. Furthermore, this study can help estimate the thermal performance of ET-CPC applications and economics and environmental impact analysis with real-time input parameters.

System description and methodology

The system presented in this research is installed on the roof and front lawn of the Department of Mechanical Engineering, Malaviya National Institute of Technology, Jaipur (26.86° N, 75.81° E). The installed ET-CPC solar field consists of 27 modules of 18 evacuated tubes each. Each ET-CPC module has an effective area of 3 m^2, and thus, a total aperture area is 81 m^2. As shown in Fig. 1, the installed ET-CPC field is arranged as six rows containing four ET-CPCs in series, and one row has three ET-CPCs in series, constituting a total aperture area of 81 m^2 with 27 ET-CPC modules. This ET-CPC solar field is in the loop with a sensible thermal energy storage tank of 2.2 m^3 capacity (containing soft water as a working medium) with the help of a centrifugal pump. Fig. 2 shows the pictorial view of the ET-CPC solar field. The technical descriptions of the ET-CPC, thermal energy storage tank, and pump are given in Table 1. There is no heating load considered for this system while in operation. Many thermocouples, resistance temperature detectors (RTDs), and flow meters have been installed at various locations in this system for data collection, as specified in Fig. 1. Recorded data have been translated and integrated with the help of a Masibus 85xx+ 16 channel data logger.

Methodology

Furthermore, a dynamic analytical model has been developed to carry out energy, exergy, environmental impact, and economic analyses of this SDWH. The values of different parameters used in this model are presented in Table 2. Subsequently, experimental validation of the model has been done using energetic efficiency and functional heat gain from this system. A parametric study is also performed to investigate the effect of the mass flow rate of the working fluid, solar radiation intensity, and ambient temperature on the productivity and efficiency of the system. Four potential locations have been identified from Rajasthan (India):

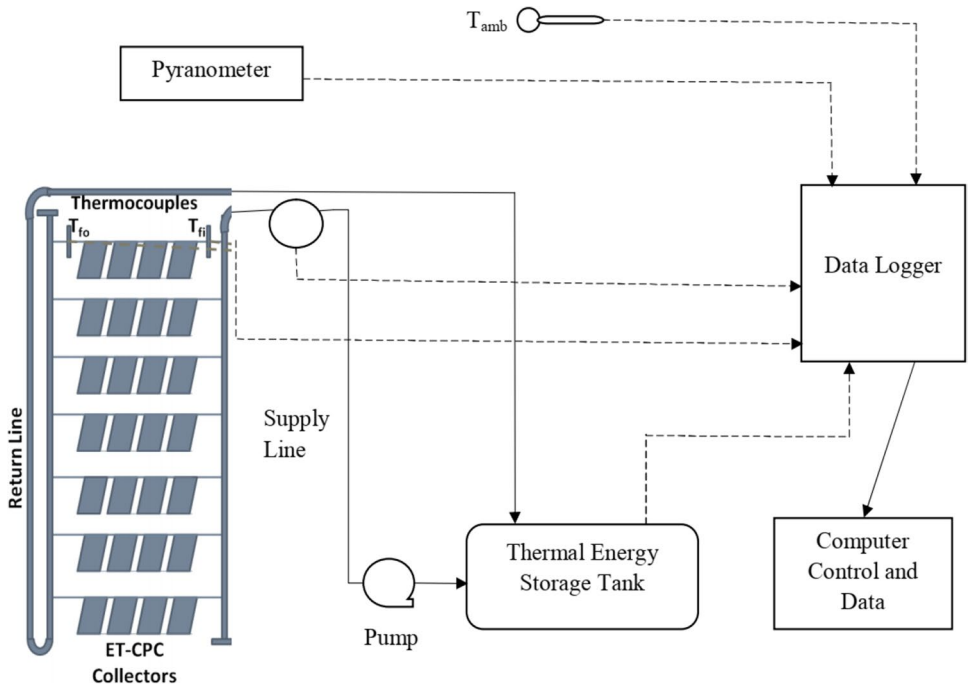

Fig. 1 Schematic diagram of evacuated tube compound parabolic concentrator solar domestic water heating system

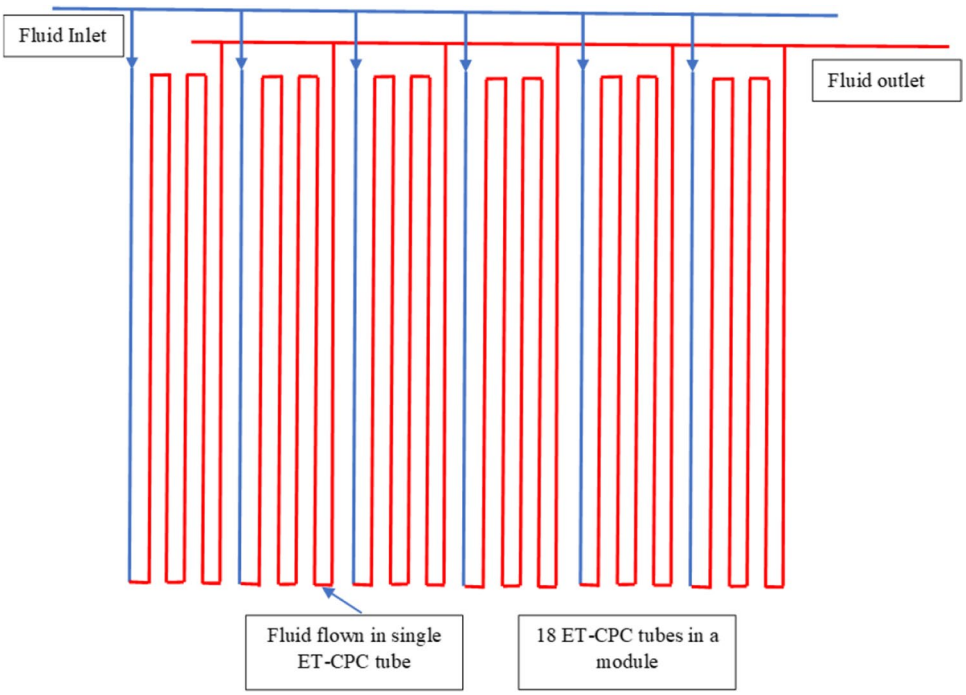

Fig. 2 Fluid flow diagram inside an ET-CPC module

Table 1 Technical description of the various components in the system

Description	Unit	Technical specification
Solar collectors		
No. of evacuated tubes	nos.	18
η_0 concerning aperture, EN12975	%	64.2
Heat transfer coefficient (a_1)	(W/m^2K)	0.89
Temperature-dependent transfer Coefficient (a_2)	(W/m^2K^2)	0.001
Grid dimensions	m	2.08 × 1.64 × 0.10
Aperture area	m^2	3.41
Max working overpressure	bar	10
Max stagnation temperature	°C	250
Glass tube material		Borosilicate glass 3.3
Selective absorber coating material		Aluminum nitride
Glass tube (Φ Ext/Φ Int/wall thickness/tube length)	mm	47/37/1.6/1500
Make		Linuo-Ritter
Hot storage tank		
Tank diameter	m	1
Tank length	m	3.5
Volume of tank	m^3	2.2
Material of tank		Mild Steel
Insulation material		Fiberglass of 50 mm thickness cladded with aluminum sheet
Orientation of tank		Horizontal
Hot water pump		
Hot water pump at 25-m head	m^3/hr	5.4

Barmer, Jodhpur, Jaisalmer, and Jaipur. The weather data for these identified locations are derived from the TMY2 file for ambient temperature and solar radiation intensity throughout the year. Energy and exergy gain, energy efficiency, and exergetic efficiency are then estimated and compared for the specified locations. As discussed earlier, no analysis can be

Table 2 Design parameters of ET-CPC field

Parameter	Value
R	0.0185 m
C_f	4186 J/kg K
L	1500 mm
A_r	0.1734 m^2
A	0.2215 m^2
$A_{c,total}$	81 m^2
n	12
τ	0.95
α	0.80
ρ_f	997 kg/m^3
$\overline{m}_f$	0.0357 (kg/s)
U_{tpa}	2.1 W/m^2 K
h_{pf}	100 W/m^2 K

conclusive without environmental and economic assessment. Therefore, environmental analysis is performed to show the amount of CO_2 emissions saved using the given system. In the later section, an economic analysis is done for comparing SDWH with the conventional water heating methods.

The following assumptions have been considered while conducting this study:

a. No heat loss from thermal energy storage and piping system has been taken into account due to thermal insulation provided.
b. The frictional pressure loss due to friction between the fluid and pipe wall is not considered.
c. Mass flow rate has been assumed to be constant.
d. A discount rate of 6% has been taken for the economic analysis along with 5% current annual growth rate for electricity prices.
e. Carbon credits have not been considered while doing economic analysis which could have provided a better cost benefit scenario.

Uncertainty analysis

The uncertainty calculated is based on the uncertainty of the instruments used to record the data as well as the error in measurement during the experiments, such as various loop inlet and outlet temperatures, solar radiation intensity, and heat transfer flow rates. The specifications of the instruments used to record the data are shown in Table 3. Also, the uncertainty and sensitivity of the instruments are mentioned. The uncertainty in the estimation of useful heat gain is calculated using the below equation:

$$\frac{\Delta Q_{useful}}{Q_{useful}} = \left[\left(\frac{\Delta m}{m}\right)^2 + \left(\frac{\Delta T}{T}\right)^2\right]^{\frac{1}{2}} \tag{1}$$

Similarly, uncertainty in the instantaneous energy efficiency is also calculated as:

$$\frac{\Delta \eta_{instantaneous}}{\eta_{instantaneous}} = \left[\left(\frac{\Delta m}{m}\right)^2 + \left(\frac{\Delta T}{T}\right)^2 + \left(\frac{\Delta I_T}{I_T}\right)^2\right]^{\frac{1}{2}} \tag{2}$$

The errors in measurements are evaluated using the method suggested by Arat et al. (2021). The average of the measured values is given as below:

$$\overline{X} = \frac{\sum X_m}{n} \tag{3}$$

where n is the number of the measurements and X_m is the measured values. Standard deviation (SD) is given as follows:

$$SD = \sqrt{\frac{\sum_{m=1}^{n}\left(X_m - X\right)^2}{(n-1)}} \tag{4}$$

Then, uncertainty (U) is given by Eq. (5) as follows:

$$U = \frac{SD}{\sqrt{n}} \tag{5}$$

The uncertainties/errors of various measured parameters and calculated values are in the range of standard limits. The uncertainty while calculating useful heat gain is ± 0.59%, and instantaneous energy efficiency is ± 1.16%. Furthermore, the estimated error in temperature measurement is ± 0.3%, useful heat gain is ± 2.5%, and instantaneous energy efficiency is ± 2.7%.

Table 3 Instruments used to record the data

Measurement type	Sensor type	Range	Uncertainty	Sensitivity
Solar radiation	Pyranometer	0–2000 W/m^2	< 1.0 %	15 μV/(W/m^2)
Fluid temperature	RTD (PT100) 3wire	− 200 to 850 °C	0.1 °C	0.385 Ω/°C
Volume flow rate	Electromagnetic (4-20 mA)	0–20 m^3/hr	±0.5%	0.059 mV/(m^3/hr)
Ambient temperature	Thermocouple (K-type)	− 200 to 1200 °C	±1.0%	41 μV/°C

Table 4 Energy analysis of evacuated tube compound parabolic concentrator

Energy analysis of ET-CPC	Eq. no.
$T_{out,n}$ outlet temperature from the n^{th} ET-CPCs coupled in series is deliberate as in (Mishra et al. 2015): $T_{out,n} = \frac{(A_c F_R \alpha\tau)_1}{\dot{m}_f C_f} \times \frac{(1-K_{eff})^n}{(1-K_{eff})} I_T + \frac{(A_r F_R U_L)_1}{\dot{m}_f C_f} \times \frac{(1-K_{eff})^n}{(1-K_{eff})} T_{amb} + K_{eff}^n T_{in}$ Where, $K_{eff} = 1 - \frac{A_r F_R U_L}{\dot{m}_f C_f}$ $F_R = \frac{\dot{m}_f C_f}{U_L A_r}\left[1 - \exp\left(-\frac{2\pi r L U_L}{\dot{m}_f C_f}\right)\right]$	6
Practical heat gain for the n-tube connected in series is given as: $Q_{useful,\,n} = (\alpha\tau)_{eff} I_T - (UA)_{eff}(T_{in} - T_{amb})$ Where, $(\alpha\tau)_{eff} = A_c F_R \alpha\tau\left(\frac{1-K_{eff}^n}{1-K_{eff}}\right)$ $(UA)_{eff} = A_r F_R U_L\left(\frac{1-K_{eff}^n}{1-K_{eff}}\right)$	7
Instantaneous thermal efficiency ($\eta_{Instantaneous}$) is given as $\eta_{Instantaneous} = \frac{Q_{useful}}{\eta_{opt} \times A_{c,total} \times I_T}$	8

Energy, exergy, environment impact, and economic analyses

Energy analysis of ET-CPC

The energy analysis for ET-CPC first involves estimating the rise in fluid inlet temperature at the exit from the ET-CPC arrays. This gain in the inlet temperature of the working fluid is calculated from the equations developed by Mishra et al. (2015). Beforehand, it is essential to be aware of the flow distribution inside an ET-CPC module; therefore, a correct assessment of the flow rate inside a tube can be done. Fig. 2 shows the flow distribution inside a single module of ET-CPC, which supports the exact number of evacuated tubes linked in series in the current setup.

The useful heat gain and energetic efficiency have been considered along with the estimation of outlet temperature from the ET-CPC solar field, and the reduced equations are presented in Table 4 for the desired energy analysis. As discussed earlier, each ET-CPC module has 18 evacuated tubes, and such four modules are connected in series to make an array. Furthermore, such 7 rows are arranged in parallel loops. Therefore, flow inside a single module is further divided into 6 sub-divisions and returned after circulating into 3 tubes inside a single module to another module connected in series. Hence, 12 tubes of 4 ET-CPC modules are connected in series. Since the total mass flow rate is divided into 7 rows and 6 subdivisions, only one fraction of forty-two of the total mass flow rate is observed inside any particular evacuated tube. Thus, only a 0.02 kg/s mass flow rate is observed inside any particular evacuated tube, whereas the actual discharge from the centrifugal pump is 0.83 kg/s, significantly less than the rated discharge of 1.5 kg/s. It is mainly because of the significant pressure drop across the ET-CPC solar field.

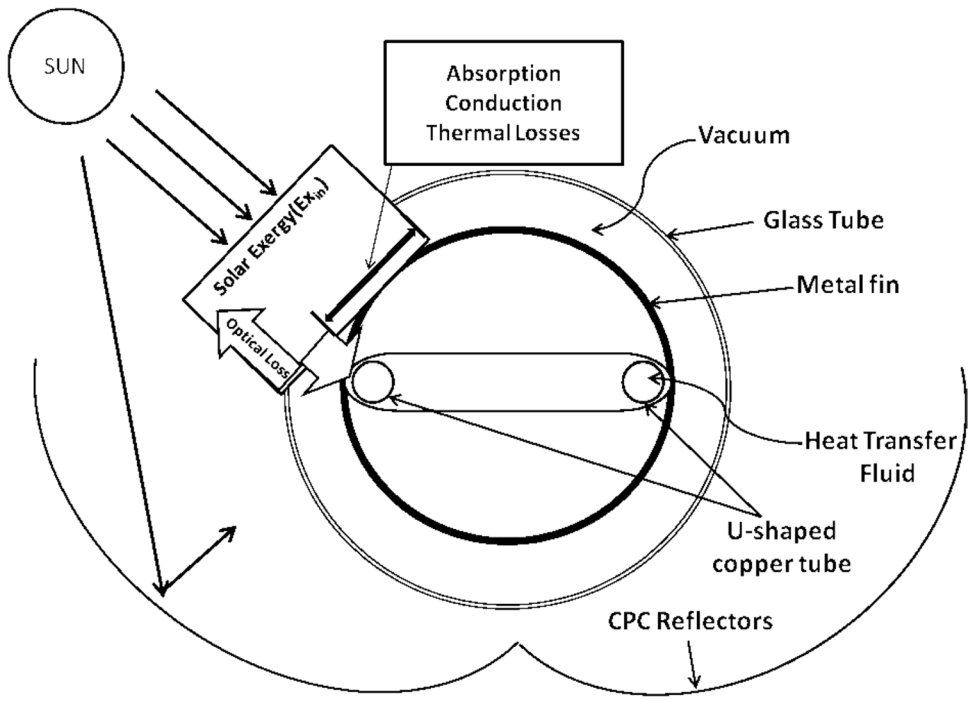

Fig. 3 Representation of various exergy destructions inside a single evacuated tube compound parabolic concentrator sub-division

Exergy analysis of ET-CPC

As discussed earlier, most of the reported research on exergy analysis of ET-CPCs considered the inlet and outlet temperatures of ET-CPCs and ambient temperature to estimate the exergy gain and exergetic efficiency. The various exergy destructions from an ET-CPC sub-division are shown in Fig. 3, while the various equations to estimate the exergy destructions, useful exergy gain, and exergetic efficiency are reported in Table 5. These models did not reflect the actual in-sights on the exergy destructions during each step of energy transitions within ET-CPCs. Thus, a dynamic mathematical model is prepared to estimate various exergy destructions while performing exergy analysis. This would help identify the exergy destruction intensive steps. The outcome of this analysis may be further helpful to better the design of ET-CPCs.

Thermodynamic analysis of thermal energy storage

Thermodynamic analysis of thermal energy storage has been performed under actual environmental conditions during the charging, storing, and discharging phases. Since the sensible thermal energy storage reported here is 2.2 m^3 in volume and oriented horizontally, a complete energy mix model is used while performing energy and exergy analyses. Furthermore, energy gain and subsequent temperature rise at any given time inside the tank are estimated as the cumulative sum of the energy gains from the ET-CPCs as per Equation (8). However, the various reduced equations for identified energy and exergy parameters have been reported below and discussed. They are analyzed in conjunction with the performance of ET-CPC.

Table 5 Exergy analysis of evacuated tube compound parabolic concentrator

Exergy analysis of ET-CPC	Eq. no.
Exergy balance equation in the steady-state condition	
$\dot{E}x_{in} = \Delta\dot{E}x_{opt} + \Delta\dot{E}x_{abs} + \Delta\dot{E}x_{thermal} + \Delta\dot{E}x_{cond} + \Delta\dot{E}x_{friction} + \dot{E}x_{useful}$	9
Exergy inlet (Petela 2003, 2005)	
$\dot{E}x_{Sun} = \dot{E}x_{in} = A_{c,total} I_T \, \phi_{solar\ rad,\max}$	10
$\phi_{Solarrad,\max} = \left[1 + \frac{1}{3}\left(\frac{T_{amb}}{T_{sun}}\right)^4 - \frac{4}{3}\left(\frac{T_{amb}}{T_{sun}}\right)\right]$	
Exergy destruction due to optical	
$\Delta\dot{E}x_{opt} = \dot{E}x_{sun}\left(1 - \eta_{opt}\right)$	11
Exergy destruction due to absorption	
$\Delta\dot{E}x_{abs} = \eta_{opt}\left(\dot{E}x_{sun} - I_T \times A_{c,total}\left(1 - \frac{T_{amb}}{T_{receiver}}\right)\right)$	12
Exergy destruction due to thermal losses	
$\Delta\dot{E}x_{thermal} = K_{loss}\left(T_{surface} - T_{amb}\right)\left(1 - \frac{T_{amb}}{T_{surface}}\right)$	13
Exergy destruction due to conduction	
$\Delta\dot{E}x_{cond} = T_{amb}\left(\Delta S_{cond}\right)$ $\Delta S_{cond} = \int_{Tin}^{Tout} \frac{\dot{m}_f C_f dT}{T} - \frac{1}{T_{receiver}} \int_{Tin}^{Tout} \dot{m}_f C_f dT$ $\Delta S_{cond} = \dot{m}_f C_f \left[\ln\left(\frac{T_{out}}{T_{in}}\right) - \left(\frac{T_{out} - T_{in}}{T_{receiver}}\right)\right]$	14
Exergy destruction due to pipe friction (Bejan et al. 1981)	
$\Delta\dot{E}x_{friction} = \frac{\dot{m}_f T_{amb} \Delta P}{\rho_f T_{in}}$ $\Delta P = f \ \rho_f \ L \frac{V^2}{2D}$ $f = \frac{64}{\mathrm{Re}}$, for $\mathrm{Re} \le 2200$ $f = 0.316\mathrm{Re}^{-0.25}$, for $\mathrm{Re} > 2200$ $\mathrm{Re} = \frac{\rho_f \ V \ D}{\mu_f}$	15
Exergy useful	
$\dot{E}x_{useful} = \dot{E}x_{in} - \left(\Delta\dot{E}x_{opt} + \Delta\dot{E}x_{abs} + \Delta\dot{E}x_{thermal} + \Delta\dot{E}x_{cond} + \Delta\dot{E}x_{friction}\right)$	16
Total exergy gain	
$Ex_{gain,total} = \int \dot{E}x_{useful}.A_{total}.dt$	17
Exergetic efficiency	
$\psi_{exergetic} = \frac{\dot{E}x_{useful}}{\dot{E}x_{in}}$	18

Table 6 Indicators of economic analysis

Economic analysis indicators/parameters	Eq. no.
Simple payback period (SPBP)	
$SPBP = \frac{CC}{CF}$	23
Discounted payback period (DPBP)	
$DPBP = \frac{\ln\left(\frac{1}{1-\frac{CC*r}{CF}}\right)}{\ln(1+r)}$	24
Internal rate of return (IRR)	
$0 = \sum_{n=1}^{N} \frac{CF_n}{(1+IRR)^n} + CI$	25
Levelized cost of heating (LCOH)	
$LCOH = \frac{TLCC}{E_n}\left[\frac{1-(1+i)^{-n}}{i}\right]$	26

$$\eta_{O,TES} = \frac{Energy\ recovered\ from\ TES\ during\ discharging}{Energy\ input\ to\ TES\ during\ charging} = \frac{\sum Q_{rec}}{\sum Q_{in,TES}} \quad (19)$$

The exergy efficiency of thermal energy storage is estimated as below:

$$\psi_{O,TES} = \frac{Exergy\ recovered\ from\ TES\ during\ discharging}{Exergy\ input\ to\ TES\ during\ charging} = \frac{\sum Ex_{rec}}{\sum Ex_{c,in}} \quad (20)$$

Environmental impact analysis

With the ever-increasing concern about the environmental impact and specifically the global warming due to greenhouse gases, it has become essential to evaluate and analyze the newly designed and developed system environmentally before heading forward. The developed system was weighed on an environmental impact basis and quantified based on savings on carbon dioxide emissions. The change resulted in significant savings in annual CO_2 and a reduced carbon footprint. The annual social cost of CO_2 emission varies from one country to another. The cost of penalty for CO_2 emissions is calculated using the relation:

$$\dot{Z}_{env} = m_{co_2}.C_{co_2} \quad (21)$$

In the above equation, C_{co_2} is the cost of unit carbon dioxide production, and it varies from 40 to 80 $/tonnes of CO_2 emissions (Team AC 2019). Here, m_{co_2} is the mass of CO_2 emission and has been calculated using emission conversion factor as follows:

$$m_{co_2} = \lambda.Energy\ Consumption(\text{kWh}) \quad (22)$$

where λ is the emission conversion factor having a value of 0.95 kg/kWh.

Economic analysis

There are indirect benefits in terms of environmental protection, lower health costs, and global climate benefits for solar-based applications such as cooling, heating, or electricity, but investments in renewable systems are never decided on these grounds. Too often, lawmakers provide incentives that can attract investment given these social benefits. Moreover, any system must sustain itself until its financial viability or beneficiary.

It is well known that fossil-based systems are relatively cheaper in terms of initial cost, but they have a higher recurring cost, including regular energy bills and maintenance costs. On the other hand, solar-based systems are characterized by high initial costs and negligible operating costs. Hence, it is essential to have a life cycle cost approach while comparing solar-based systems with fossil-based systems.

The concept of life cycle cost includes both initial investment costs and year-to-year operating costs in economic

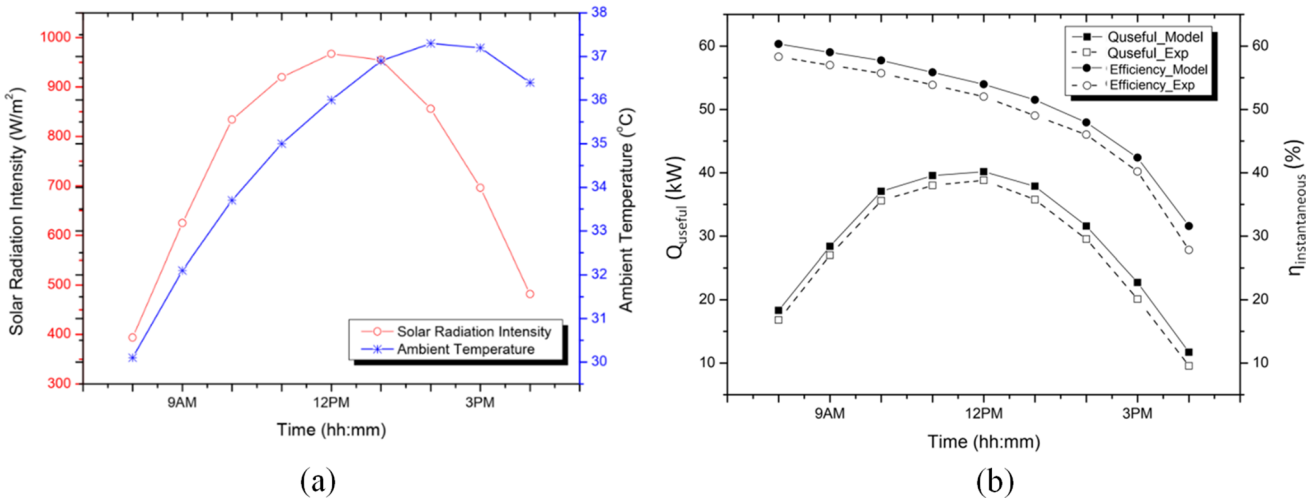

Fig. 4 Experimental validation of analytical model on a typical day, April 18, 2021. **a** Solar radiation intensity and ambient temperature, **b** efficiency and Q_{useful} model and experimental

decision-making. The life cycle cost of any energy system is the sum of the following costs incurred over its lifetime:

1. First cost (cost of equipment, installation, cost of land, etc.)
2. Running/operation cost
3. Interest/depreciation
4. Maintenance cost
5. Taxes
6. Salvage value

The solar-based systems are typically evaluated economically using various factors such as simple/discounted payback periods (SPBPs/DPBPs) and internal rate of return (IRR). Various financial performance parameters are analyzed over here (refer to Table 6).

Results and discussion

A dynamic analytical model of energy, exergy, environmental impact, and economic analyses has been developed for the solar domestic water heating system powered by the ET-CPC solar field. Firstly, the reported model is validated with the experimental data. Furthermore, parametric studies have been reported to understand the effect of various input parameters on the performance and productivity of the ET-CPC solar field. The energy and exergy parameters have been estimated with the help of a developed dynamic analytic model using real-time physical conditions of four different locations in Rajasthan (India). The latter section presents various indicators for reporting environmental impact and economic analysis.

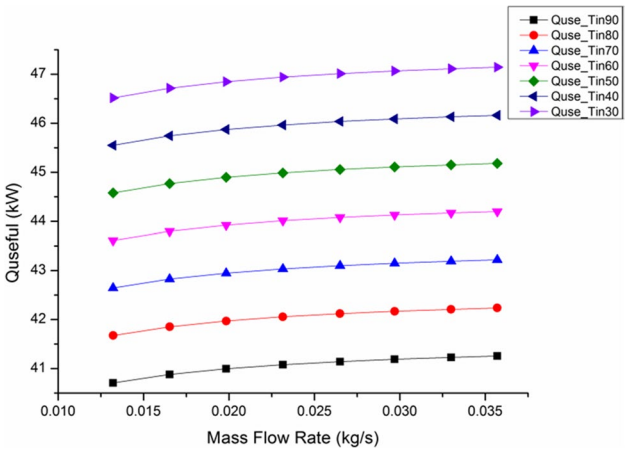

Fig. 6 Effect of mass flow rate on useful heat gain at different inlet temperatures

Experimental validation of analytical model

Experimental validation is carried out to validate the developed model developed for a typical solar day. The experimental data are recorded while accumulating thermal energy converted from solar energy using ET-CPC solar field within the integrated sensible thermal energy storage. It is observed from this experimental validation that relative differences are within the range of 3 to 8% (refer to Fig. 4). Thus, there is a good agreement between the values from the dynamic analytical model and experimental results.

Parametric analysis

This parametric study aims to show the effect of mass flow rate, solar radiation intensity, and ambient temperature on the productivity and efficiency of the ET-CPC solar field in

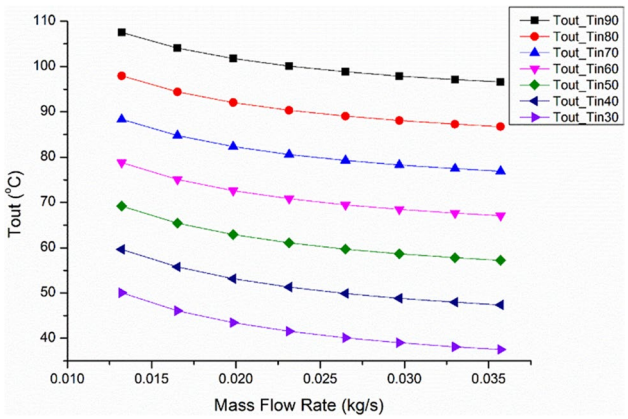

Fig. 5 Effect of mass flow rate on outlet temperature at a different inlet temperature

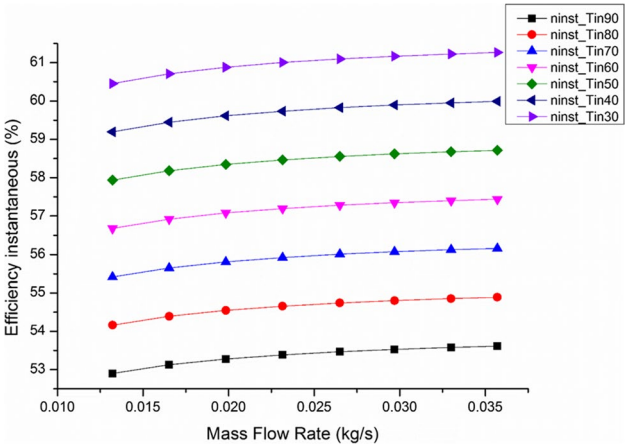

Fig. 7 Effect of mass flow rate on instantaneous efficiency with different inlet temperatures

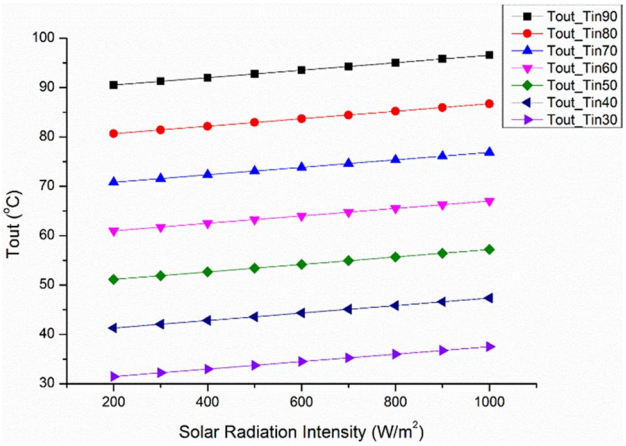

Fig. 8 Variation of the outlet temperature as a function of the solar radiation intensity for various inlet temperatures

conjunction with sensible thermal energy storage. A typical range of mass flow rate is taken from 0.013 to 0.036 kg/s through tubes of ET-CPC. The solar radiation intensity values vary from 200 to 1000 W/m^2 in the steps of 100 W/m^2, whereas ambient temperature values range from 27 to 43°C.

Effect of mass flow rate

The effect of mass flow rate is shown on the outlet temperature of heat transfer fluid from the ET-CPC solar field, as shown in Fig. 5. The solar radiation intensity has been kept at 1000 W/m^2, while the ambient temperature is 27 °C (Zielińska et al. 2018). The temperature of the heat transfer fluid at the inlet has varied from 30 to 90 °C within the steps of 10 °C. It is observed from the study that the temperature of heat transfer fluid decreases with the increase in the mass flow rate, which supports the previous literature. For inlet temperature of 30 °C, the slope of the curve is steepest, while for inlet temperature of 90 °C, the slope of the curve is less steep.

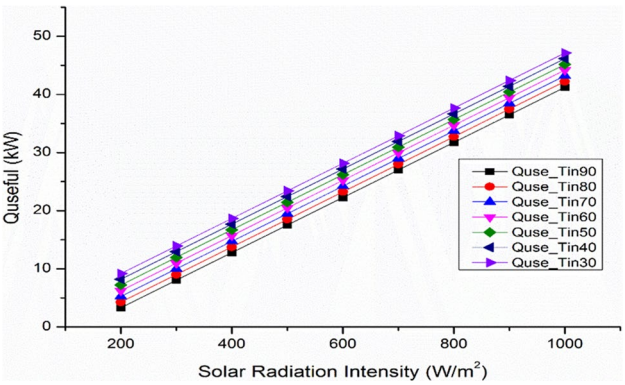

Fig. 9 Effect of solar radiation intensity on useful heat gain

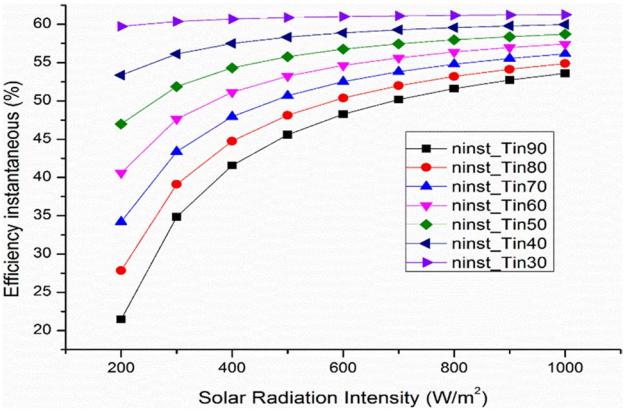

Fig. 10 Effect of solar radiation intensity on instantaneous efficiency

Similarly, the effect of mass flow rate on the useful heat gain is reported at different inlet temperatures in Fig. 6. The intensity of solar radiation is 1000 W/m^2, and the ambient temperature is kept at 27 °C. It is observed that useful heat gain increases proportionally with the mass flow rate. Moreover, Q_{useful} is more at low inlet temperatures and vice-versa for high inlet temperatures, mainly due to high heat loss to the environment at high temperatures.

Furthermore, the effect of mass flow rate over instantaneous efficiency of ET-CPC for various inlet temperatures is shown in Fig. 7. As previously, solar radiation intensity and ambient temperature are taken as constant. The instantaneous efficiency of the system improves with the increase in mass flow rate. It is also noted that instantaneous efficiency is more for low inlet temperatures and decreases as the temperature increases. This is mainly because of increasing heat loss to the environment at elevated temperatures. It is also well known that keeping

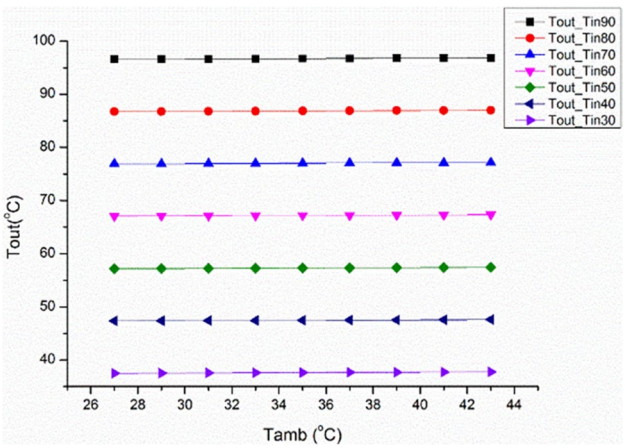

Fig. 11 Effect of ambient temperature on outlet temperature with different inlet temperatures

the mass flow rate low allows the outlet temperature to reach high, which ultimately increases the heat losses and reduces the useful heat gain and instantaneous efficiency of ET-CPC.

Effect of solar radiation intensity

The solar radiation intensity is a significant and most influential input parameter. The solar radiation intensity ranges from 200 to 1000 W/m^2 taking constant ambient temperature of 27 °C and mass flow rate of 0.036 kg/s. The effect of solar radiation intensity on outlet temperature is shown in Fig. 8. There is a noticeable increase in the fluid outlet temperature corresponding to the increase in the solar radiation intensity. Thereafter, the effect of solar radiation intensity is presented in Fig. 9. The useful heat gain continues to increase with the increase in solar radiation intensity while it is highest for an inlet temperature of 30 °C. However, it continues to decrease with increasing the heat transfer fluid inlet temperature. For the given system, useful heat gain is between 40 and 46 kW for a solar radiation intensity of 1000 W/m^2 at various inlet temperatures.

Furthermore, the effect of solar radiation intensity on the instantaneous efficiency of the ET-CPC solar field for various inlet temperatures is shown in Fig. 10. The instantaneous efficiency increases with the increase in the solar radiation intensity, while it is highest at 30 °C inlet temperature and solar radiation intensity of 1000 W/m^2. At lower levels of solar intensity, the instantaneous efficiency range widens, but as solar intensity increases, this difference narrows. Furthermore, it can be observed that instantaneous efficiency

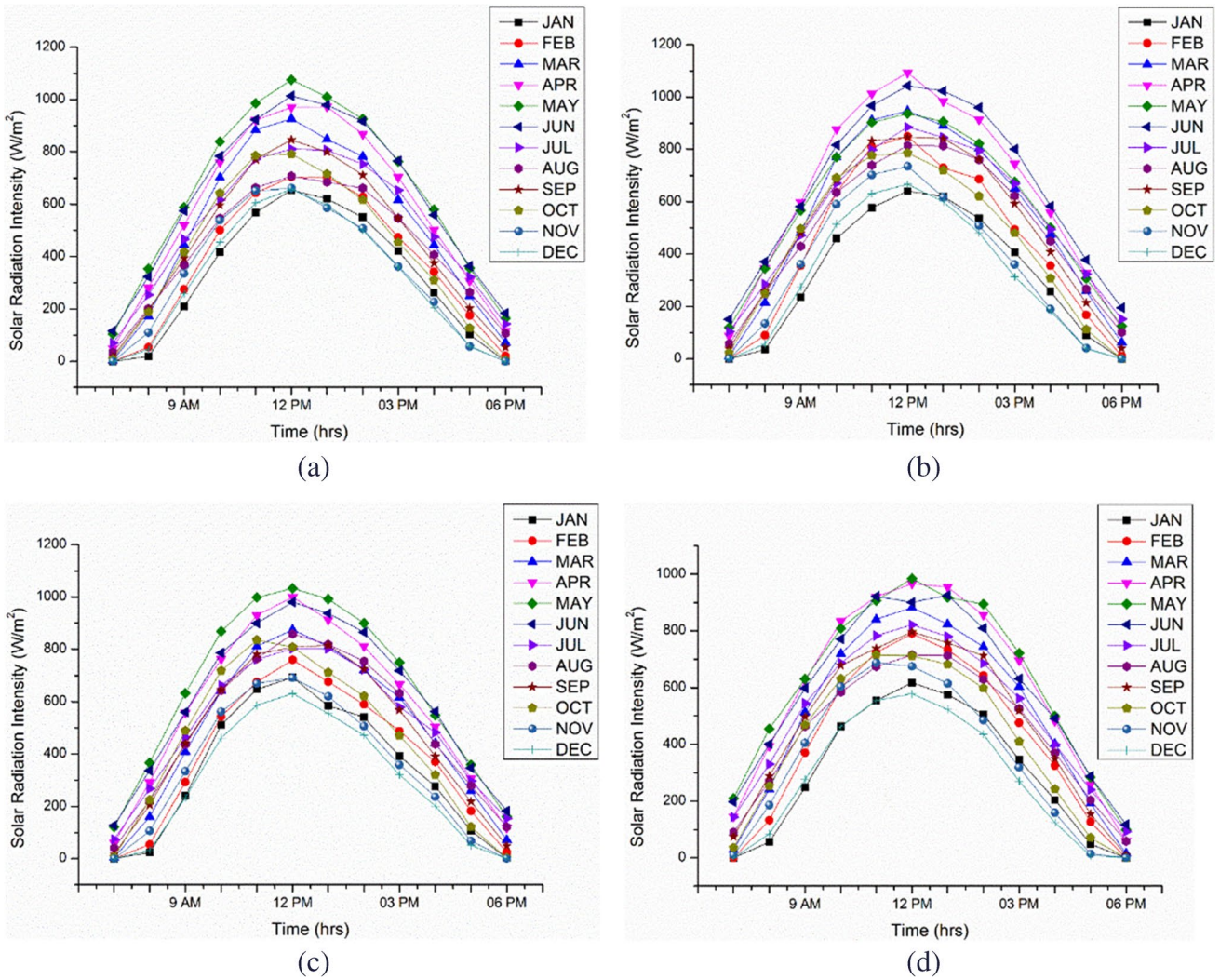

Fig. 12 Solar radiation intensity data for **a** Barmer, **b** Jodhpur, **c** Jaisalmer, **d** Jaipur

is still in the range of 45–60%, which is significantly better than any other stationary STC.

Effect of ambient temperature

The effect of ambient temperature on productivity is discussed in this section. The solar radiation intensity is 1000 W/m^2, while a mass flow rate of 0.036 kg/s is considered. The effect of ambient temperature over fluid outlet temperature for various inlet temperatures is shown in Fig. 11. No significant change in the outlet temperature of the heat transfer fluid is observed with the increase in ambient temperature. Hence, it can be concluded from this discussion that ambient temperature is the least dominant factor which affects the productivity of ET-CPC and, similarly, useful heat gain and instantaneous efficiency.

Estimation of useful energy and exergy gain under actual meteorological conditions

As mentioned earlier, the developed dynamic analysis is used to estimate the energy and exergy gains and efficiencies under the meteorological conditions of four potential locations in Rajasthan (India) with the help of a TMY2 data file. The real-time physical data have been used in the reported model for the mentioned ET-CPC-powered SDWH system. In this study, various energy and exergy analysis indicators such as useful heat gain, instantaneous efficiency, useful exergy gain, and exergetic efficiency have been chosen.

The solar radiation intensity variation for a typical year is presented in Fig. 12a, b, c, and d for Barmer, Jodhpur, Jaisalmer, and Jaipur, respectively. The maximum solar radiation intensity levels are recorded from April to June, while the lowest is recorded between November and January. The highest value of solar intensity is recorded as 1075, 1093, 1033 and 985 W/m^2 for Barmer, Jodhpur, Jaisalmer, and

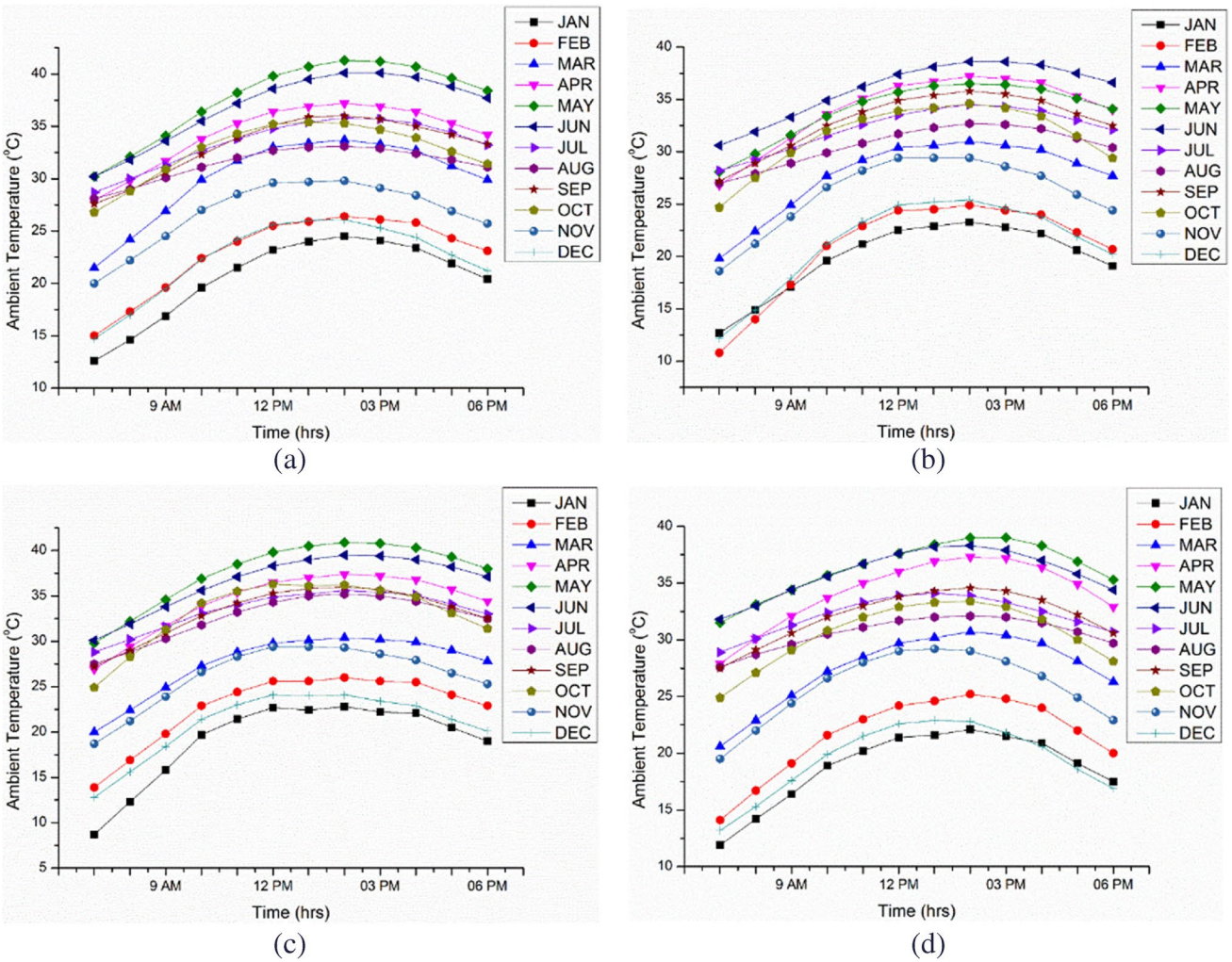

Fig. 13 Ambient temperature data for **a** Barmer, **b** Jodhpur, **c** Jaisalmer, **d** Jaipur

Jaipur, respectively. The highest solar intensity is observed almost every month at around 12 noon.

Similarly, Fig. 13a, b, c, and d show the variation of ambient temperatures for a typical year for Barmer, Jodhpur, Jaisalmer, and Jaipur, respectively. The highest ambient temperature is achieved during May, while the lowest is in January and around 2 pm every month. The maximum ambient temperature for Barmer, Jodhpur, Jaisalmer, and Jaipur is recorded as 41.3, 38.5, 40.9, and 39 °C, respectively, while the lowest temperature recorded is 15 °C for Jaisalmer. The warmest months for all specified locations are May, June, and July, while the coldest months are December, January, and February.

Energy analysis

The comparative analysis of solar radiation intensity, useful heat gain, and instantaneous efficiency for different months under the meteorological condition of Barmer is presented in Fig. 14a. Similarly, Fig. 16b, c, and d show the useful heat gain, instantaneous efficiency, and solar radiation intensity for different months at Jodhpur, Jaisalmer, and Jaipur locations, respectively. The useful heat gain curve shows maximum values during April and May for all locations. Furthermore, it is seen from Fig. 14 that the solar radiation intensity and Q_{useful} shows higher values during the summer months, while the instantaneous efficiency curve shows higher values for the winter months. It is mainly due to the significant temperature differences between the inlet and outlet temperature of heat transfer fluid during the winter months, and energy efficiency is directly proportional to this temperature difference.

The highest solar radiation intensity is 1093 W/m^2 for Jodhpur during April and May, followed by 1033 and 985 W/m^2 for Jaisalmer and Jodhpur locations. The highest value of Q_{useful} is recorded as 46.02 kW for Jodhpur followed by 42.86 and 40.67 kW for Jaisalmer and Jaipur, respectively, during April and June. Similarly, the highest value of instantaneous efficiency is recorded for Jodhpur as 67.25% during January, followed by 67.14 and 66.53% for Jaisalmer and Jodhpur, respectively. Similarly, the highest instantaneous efficiency recorded for Jodhpur is 67.25%

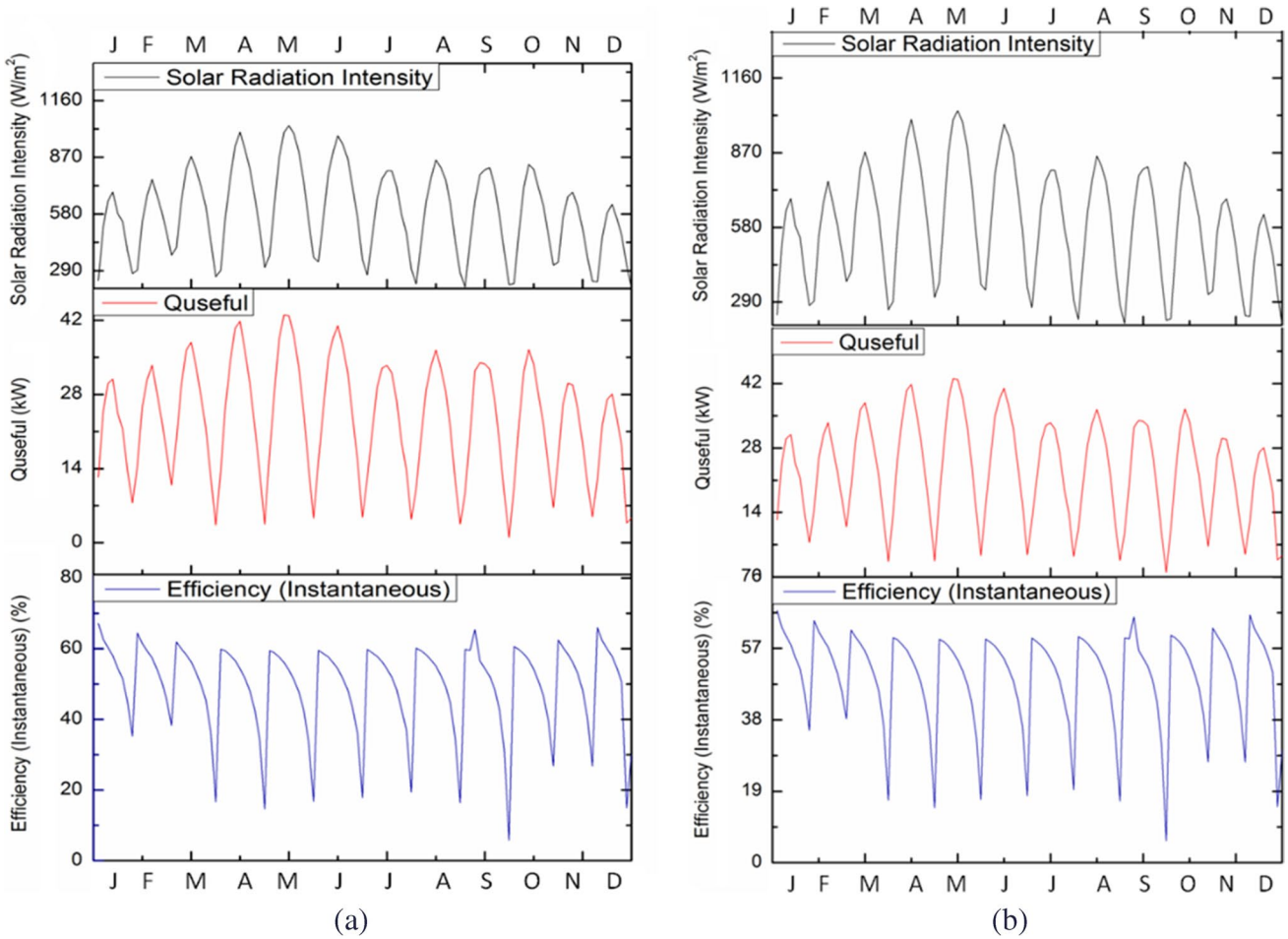

Fig. 14 Parameters indicating energy analysis under the meteorological conditions of **a** Barmer, **b** Jodhpur, **c** Jaisalmer, **d** Jaipur

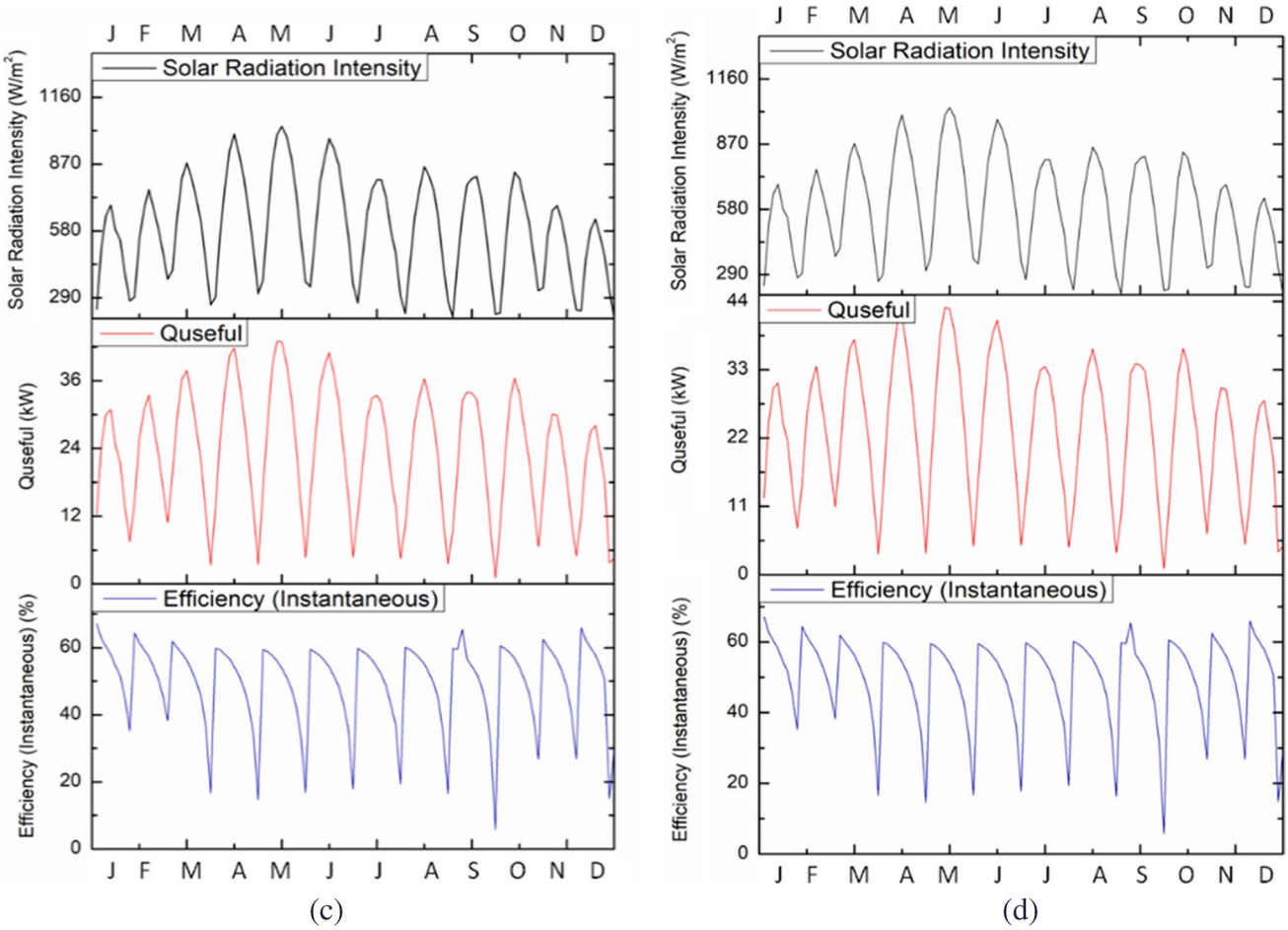

Fig. 14 (continued)

during January, followed by 67.14 and 66.53% for Jaisalmer and Jodhpur, respectively. Accordingly, the Q_{useful} is estimated to be higher for April, May, and June for all four locations identified.

Exergy analysis

As discussed earlier, exergy analysis refers to a qualitative assessment of energy transactions. Therefore, the exergy inlet, useful exergy gain, and exergetic efficiency have been identified as indicators of the exergy analysis of this system. These parameters have been analyzed under the meteorological conditions of identified four locations; see Fig. 15a, b, c, and d. The first part of the curves elucidates the exergy variations around the year. The maximum exergy inlet is 80.74 kW during May month at the Jodhpur location.

Furthermore, it may also be noted that the amount of exergy inlet is high in the summer season and less in the winter season. This is mainly due to the higher values of solar radiation intensity in the summer months compared to the winter months. The second and third parts of these curves illustrate the behavior of useful exergy gain and exergetic efficiency for specified locations. Higher values of useful exergy gain are observed between April and June. Maximum useful exergy gain is observed as 7.50 kW for Jodhpur followed by 7.33, 7.17, and 7.09 kW for Barmer, Jaisalmer, and Jaipur, respectively, during May.

Furthermore, the maximum exergetic efficiency is recorded for Jodhpur as 11. 05% followed by Barmer, Jaisalmer, and Jaipur as 10.58, 10.57, and 10.55%, respectively. However, there is no noticeable difference between the exergetic efficiency of all specified locations, as seen in Fig. 15.

Henceforth, a comparison is shown in Fig. 16 to discuss the quantitative and qualitative assessment of energy transactions for the SDWH powered by ET-CPC solar field for the specified locations. Comparisons have been made for annual solar energy received, useful heat gain, exergy inlet, and useful exergy gain for various specified locations. As shown in Fig. 18, Jodhpur has the most received excellent solar radiation, 162 MWh/year, and the maximum annual useful energy and exergy gain as 79.72 MWh/year and 9.311 MWh/year, respectively. Furthermore, Jaisalmer receives 157.85

MWh/year of solar radiation, converted to 76.90 MWh/year of useful energy gain, while exergy gain is estimated as 8.53 MWh/year compared to exergy inlet of 146.63 MWh/year. Similarly, useful heat gain is estimated as 75.92 and 75.32 MWh/year for Barmer and Jaipur, respectively, while exergy gain is estimated at 8.4 and 8.32 MWh/year. A comparison of various output parameters reported has been reported in Table 7 for various specified locations. Previous literature also claims to have an instantaneous energy efficiency ranging around 48%, whereas exergetic efficiency ranges from 4.7 to 7% (Gang et al. 2012).

Environmental impact analysis

The use of solar energy is highly impactful in addressing environmental impact issues related to CO_2 emissions such as global warming, smog, acid rain, and an increase in average global ambient temperature. Therefore, CO_2 emission saving potential is estimated compared to the other existing conventional solar water heating solutions, as shown in Fig. 17. Environmental impact analysis favors using the SHWH powered by ET-CPC solar field, which saves 78.1, 75.4, 74.4, and 73.8 tonnes of CO_2 emissions for Jodhpur, Jaisalmer, Barmer, and Jaipur, respectively, which could have been added to the environment if the electricity was used for the same purpose.

Economic analysis

Economic analysis is essential for comparing various existing water heating solutions based on the profitability index. Therefore, various economic indicators have been used to report the cost-benefit analysis. For this purpose, five conventional fuel-based water heating systems have been compared with the existing solar water heating system. Table 8 shows the different fuels used for water heating and their

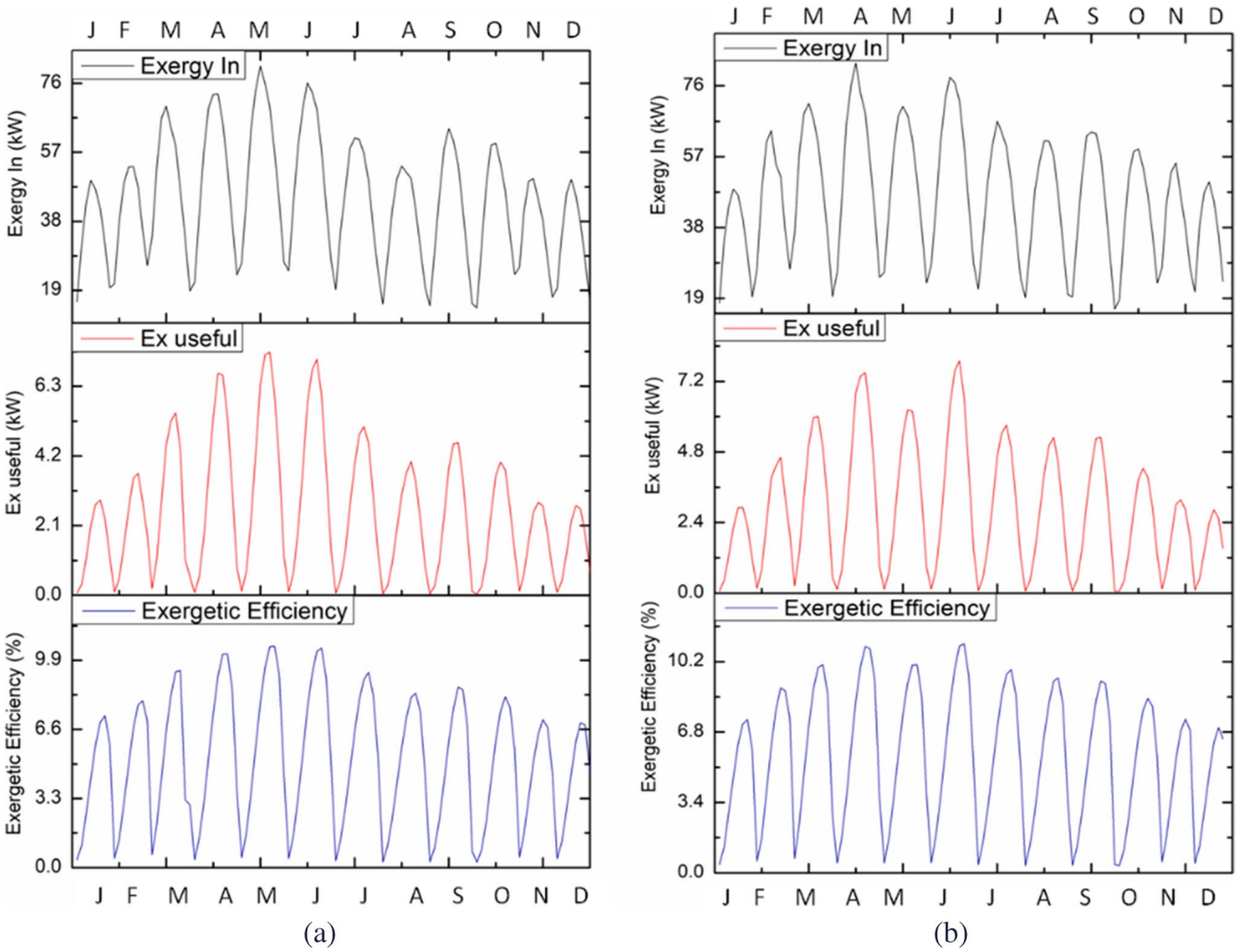

Fig. 15 Parameters indicating exergy analysis under the meteorological condition of **a** Barmer, **b** Jodhpur, **c** Jaisalmer, **d** Jaipur

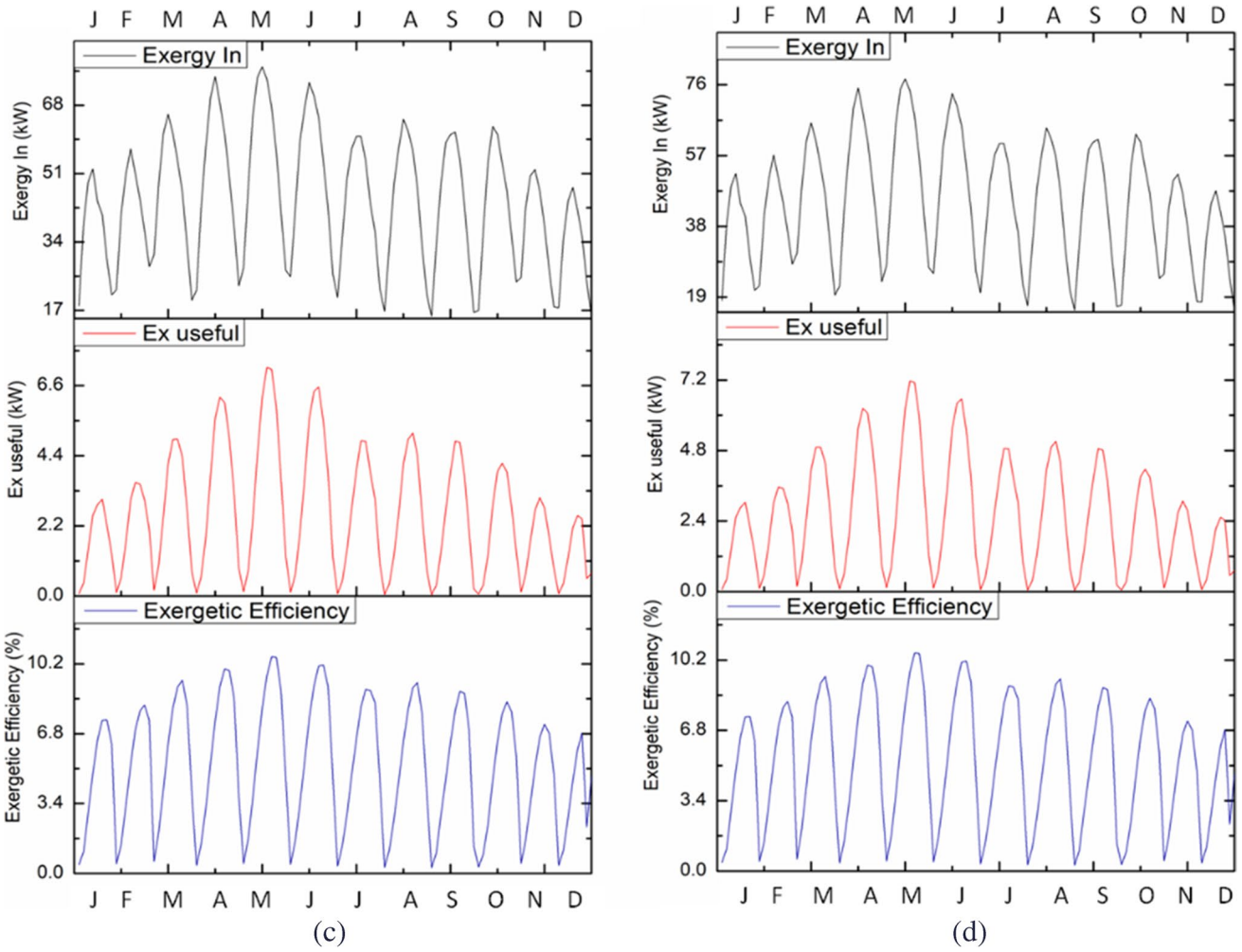

Fig. 15 (continued)

corresponding conversion efficiency, price, and calorific value of fuels used.

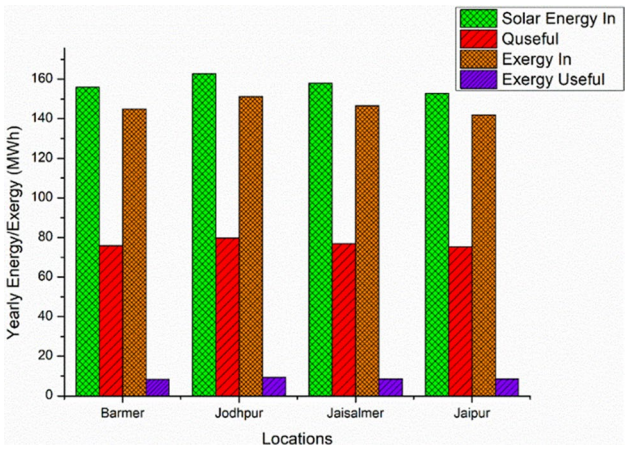

Fig. 16 Solar energy-exergy graph comparison for four different meteorological conditions

It can be easily identified that the first cost of a solar water heating system is significantly higher than that of other systems. As discussed earlier, the first cost of the solar-based water heating systems is significantly high compared to various existing conventional water heating systems. Thus, a comparison of the first cost of various water heating systems is shown in Table 9. Furthermore, annual operation and maintenance cost for various water heating systems is reported and compared in Table 10. A comparison of operation and maintenance costs has also been shown in Fig. 18. The kerosene fuel–operated water heating system shows the highest cost of operation and maintenance, followed by electricity and LPG. Hence, it can be seen that solar energy has significantly less operation and maintenance costs than other conventional fuels reported.

In addition to this, Table 11 shows the estimated life expectancy of the selected water heating systems. Thus, a detailed economic analysis is carried out based on the

Table 7 Comparative analysis of useful heat gain, instantaneous energy efficiency, useful exergy gain, and exergetic efficiency for specified locations

Location	Useful Heat Gain (kW)			Instantaneous Energy Efficiency (%)			Useful Exergy Gain (kW)			Exergetic Efficiency (%)		
	Min	Max	Avg.	Min	Max	Avg.	Min	Max	Avg.	Min	Max	Avg.
Barmer	0.56	45.09	23	3.59	67.25	49.61	0.04	7.33	2.54	0.25	10.57	5.14
Jodhpur	0.28	46.02	24.60	1.7	66.64	49.98	0.06	7.89	2.87	0.34	11.05	5.55
Jaisalmer	0.98	43.02	23.47	5.8	67.14	49.71	0.04	7.17	2.61	0.27	10.53	5.27
Jaipur	0.66	40.68	23.24	3.3	67.45	49.86	0.04	7.09	2.62	0.18	10.55	5.41

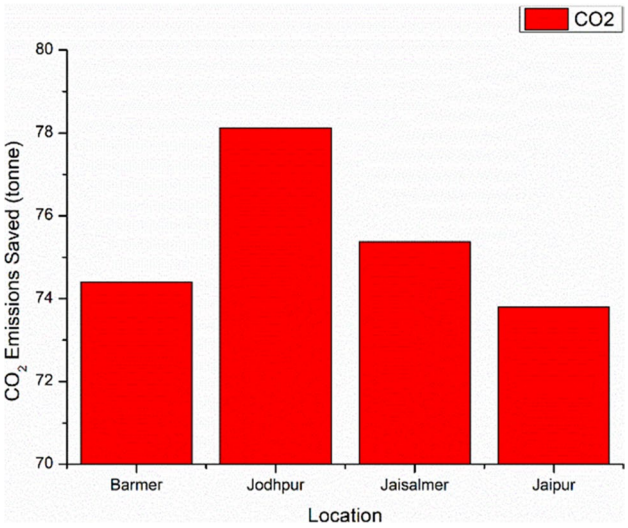

Fig. 17 Comparison of CO_2 emission saved with the use of solar energy for identified locations

Table 9 Comparison of first cost for various water heating systems

System	First cost ($)
ET-CPC solar water heating	12500
Electricity based water heater	3300
LPG/Kerosene/CNG operated water heaters	3000
Firewood operated water heater	3300

equations of identified parameters mentioned in Table 6. The internal rate of return (IRR), simple payback period (SPBP), and discounted payback period (DPBP) for various selected water heating systems are described in Table 12. SPBP and DPBP are calculated by taking a discount rate of 6%. The IRR is 16.82% for Jodhpur, followed by 16.77, 16.76, and 16.75% for Jaipur, Barmer, and Jaisalmer. Furthermore, SPBP is 4.49, 4.65, 4.72, and 4.75 years for Jodhpur, Jaipur, Barmer, and Jaisalmer, respectively, whereas DPBP ranges from 6.6 to 7.09 years.

The levelized cost of heating (LCOH) is an effective indicator for comparing the overall cost of heating per kWh of heat between various water heating systems. Therefore, a comparison of LCOH is described in Fig. 19 for various water heating systems reported here. It can be seen that the LCOH for SDWH powered by ET-CPC solar field is relatively less which is ranging from 0.022 to 0.023 $/kWh of heating, followed by kerosene (0.18 $/kWh) and electricity (0.15 $/kWh). The excellent IRR values are calculated from this economic analysis for SDWH, making it clear that it is a very profitable business model (refer to Table 12).

Conclusions and future directions

An SDWH powered by an 81-m^2 ET-CPC solar collector field is presented here. Energy, exergy, environmental impact, and economic analyses are carried out using a developed dynamic analytical model for four specified locations from Rajasthan (India). The following points are drawn as the conclusion of this work.

- The developed dynamic analytical model results are validated with experimental results, and the relative difference ranges from 3 to 8%.
- Parametric analysis shows that with an increase in the mass flow rate from 0.0132 to 0.0357 kg/s, the useful

Table 8 Comparison of price, conversion efficiency, and calorific values for various fuels

Sr. no.	Fuel	Units	Price ($)	Conversion efficiency	CV fuel (MJ/kg)
1	Electricity	per kWh	0.13	0.9	3.6 (MJ/unit)
2	LPG (2022)	per kg	0.87	0.6	55
3	Kerosene (2022)	per kg	0.86	0.4	45
4	Fuelwood	per kg	0.13	0.25	22
5	Natural gas (2021)	per kg	0.45	0.6	50

Table 10 Operation and maintenance cost for various locations for different fuels

Sr. no.	Fuel	Units	Price ($)	Conversion efficiency	CV Fuel (MJ/kg)	O&M cost ($)			
						Barmer	Jodhpur	Jaipur	Jaisalmer
1	Electricity	Per kWh	0.13	0.9	3.6 (MJ/kWh)	11060	11614	11635	10972
2	LPG	Per kg	1.2	0.6	55	9528	10005	9652	9453
3	Kerosene	Per kg	0.9	0.4	45	13692	14374	13871	13584
4	Fuelwood	Per kg	0.13	0.25	22	6621	6953	6707	6569
5	Natural gas	Per kg	0.5	0.6	50	4151	4359	4206	4119

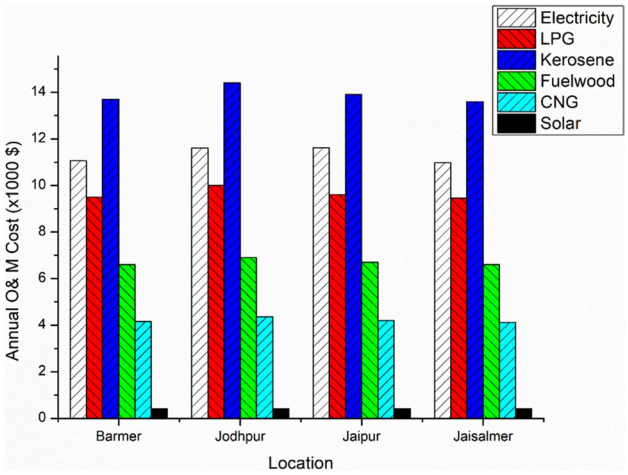

Fig. 18 Comparison of annual operational and maintenance costs for various fuels used for domestic water heating system

Table 11 Life expectancy of equipment

Expected life (solar system)	15 years
Expected life (electricity heating system)	15 years
Expected life (LPG/CNG/kerosene fired heating system)	15 years
Discount rate	6% annual

heat gain and instantaneous efficiency of the ET-CPC improved simultaneously. However, useful heat gain and instantaneous efficiency decline with an increase of 30–90 °C in the inlet temperature.

Table 12 Comparison of internal rate of return and payback periods for identified locations for solar water heating system

	IRR(%)	SPBP (Yr)	DPBP (Yr)
Barmer	16.76	4.7169	7.024
Jodhpur	16.82	4.492	6.615
Jaipur	16.77	4.656	6.912
Jaisalmer	16.75	4.7543	7.093

- The effect of solar radiation intensity ranging from 200 to 1000 W/m^2 is estimated for different inlet temperatures on the useful heat gain and instantaneous efficiency of the ET-CPC solar field.
- It has also been reported that there is no significant effect of ambient temperature over the useful heat gain and efficiency.
- Annual energy and exergy gains have been estimated and compared using a developed dynamic analytical model under meteorological conditions of four specified locations (Barmer, Jodhpur, Jaisalmer, and Jaipur). Jodhpur is receiving the most excellent solar radiation, and thus, the highest annual useful energy and energy gain has been reported to be 79.72 MW and 9.311 MW, followed by Jaisalmer, Barmer, and Jaipur.
- Economic analysis shows a simple payback period of 4.5 to 4.75 years and discounted payback period of 6.6 to 7 years based on a discount rate of 6%.
- Furthermore, solar energy costs about 0.022 $/kWh of heat, estimated based on the levelized cost of heating, compared to using CNG as fuel, which costs about 0.059 $/kWh. The highest levelized cost of heating has been

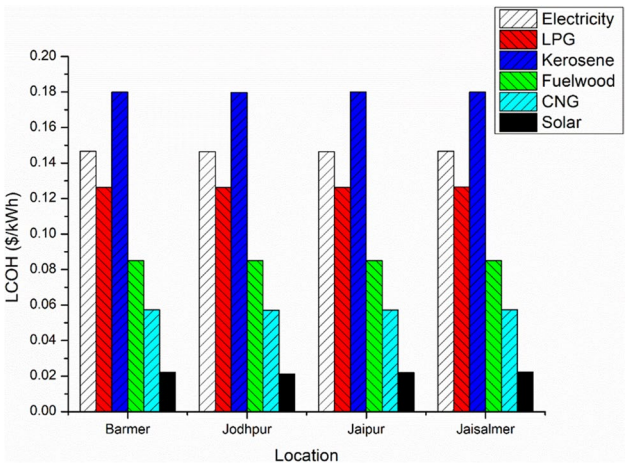

Fig. 19 Comparison of levelized cost of heating for various fuels for identified locations

reported while using electricity for domestic water heating, which is approximately 0.15 $/kWh.

- The internal rate of return for Barmer, Jodhpur, Jaipur, and Jaisalmer has been reported as 16.76, 16.82, 16.77, and 16.75%, respectively, which proves that it is a very profitable business model.
- Environmental impact analysis also favors ET-CPC, which saves 74.4, 78.1, 75.4, and 73.8 tonnes of CO2 saved, which got added to the environment if the electricity was used for the same purpose.

Hence, it can be recommended that ET-CPC is a viable, economical, and pollution-free alternative to meet the medium temperature heat demand, such as in solar water heating systems for domestic and community use. ET-CPC operation is not possible during weak sunshine (< 200 W/m^2) hours, and technological advancement is needed in this direction. The reported dynamic analytical model cannot accommodate many factors that may affect the performance of ET-CPC, such as relative humidity of the environment and dust. Furthermore, the use of nanofluids as working fluid has been reported to be beneficial to improving the productivity and performance of ET-CPCs further, but there is insufficient data, and it also reports operational issues. Furthermore, research can be done to find the optimal configuration of nanofluids to minimize operational issues and optimum performance. The sustainability of such technologies may be further highlighted by performing exergoeconomic, enviroeconomic, exergoenvironmental, and life cycle cost analyses, which are decisive in the technology selection for the future.

Acknowledgments The authors are very thankful to the Department of Science and Technology, New Delhi, for sponsoring the project DST/SSTP/Rajasthan/389 to Malaviya National Institute of Technology, Jaipur.

Author contribution Dinesh Kumar Sharma: Writing-original draft, writing (review and editing), experimentation, numerical analysis, conceptualization.

Dilip Sharma: Supervision, methodology, formal analysis, visualization.

Ahmed Hamza H Ali: Supervision, validation, formal analysis

Data availability Data available on request from the authors.

Declarations

Ethics approval This material is the authors' own original work, which has not been previously published elsewhere. The paper is not currently being considered for publication elsewhere. The paper reflects the authors' own research and analysis in a truthful and complete manner.

Consent to participate There is no such information involved in this research which requires permission; references are properly cited for mentioned information.

Consent for publication Authors disclose that there is no such information involved in this research.

Competing interests The authors declare no competing interests.

References

Aghbashlo M, Tabatabaei M, Soltanian S, Ghanavati H (2019) Biopower and biofertilizer production from organic municipal solid waste: an exergoenvironmental analysis. Renew Energy 143:64–76. https://doi.org/10.1016/j.renene.2019.04.109

Arat H, Arslan O, Ercetin U, Akbulut A (2021) Experimental study on heat transfer characteristics of closed thermosyphon at different volumes and inclination angles for variable vacuum pressures. Case Stud Thermal Eng 26:101117. https://doi.org/10.1016/j.csite.2021.101117

Arslan O, Kilic D (2021) Concurrent optimization and 4E analysis of organic Rankine cycle power plant driven by parabolic trough collector for low-solar radiation zone. Sustain Energy Technol Assess 46:101230. https://doi.org/10.1016/j.seta.2021.101230

Battisti R, Corrado A (2005) Environmental assessment of solar thermal collectors with integrated water storage. J Clean Prod 13(13-14):1295–1300. https://doi.org/10.1016/j.jclepro.2005.05.007

Bejan A, Kearney DW, Kreith F (1981) Second law analysis and synthesis of solar collector systems. J Solar Energy Eng Trans ASME 103(1):23–28. https://doi.org/10.1115/1.3266200

Bellos E, Tzivanidis C, Tsifis G (2017) Energetic, exergetic, economic and environmental (4E) analysis of a solar assisted refrigeration system for various operating scenarios. Energy Convers Manag 148:1055–1069. https://doi.org/10.1016/j.enconman.2017.06.063

Boukelia TE, Arslan O, Bouraoui A (2021) Thermodynamic performance assessment of a new solar tower-geothermal combined power plant compared to the conventional solar tower power plant. Energy 232:121109. https://doi.org/10.1016/j.energy.2021.121109

Caliskan H (2017) Energy, exergy, environmental, enviroeconomic, exergoenvironmental (EXEN) and exergoenviroeconomic (EXENEC) analyses of solar collectors. Renew Sust Energ Rev 69:488–492. https://doi.org/10.1016/j.rser.2016.11.203

Cengel YA, Boles MA, Kanoglu M (2019) Thermodynamics: an engineering approach 9th editon (SI Units). McGraw Hill, New York

Chopra K, Tyagi VV, Pandey AK, Ma Z, Ren H (2021) Energy, exergy, enviroeconomic & exergoeconomic (4E) assessment of thermal energy storage assisted solar water heating system: Experimental & theoretical approach. J Energy Storage 35:102232. https://doi.org/10.1016/j.est.2021.102232

CNG Price in India (2021) https://www.mypetrolprice.com/cng-price-in-india.aspx. Accessed 7 Dec 2021

Dincer I, Rosen MA (2007) Exergy: Energy, environment and sustainable development. Elsevier Science, Amsterdam

Faizal M, Saidur R, Mekhilef S, Hepbasli A, Mahbubul IM (2015) Energy, economic, and environmental analysis of a flat-plate solar collector operated with SiO2nanofluid. Clean Techn Environ Policy 17(6):1457–1473. https://doi.org/10.1007/s10098-014-0870-0

Gang P, Guiqiang L, Xi Z, Jie J, Yuehong S (2012) Experimental study and exergetic analysis of a CPC-type solar water heater system using higher-temperature circulation in winter. Sol Energy 86(5):1280–1286. https://doi.org/10.1016/j.solener.2012.01.019

Geete A, Dubey A, Sharma A, Dubey A (2019) Exergy analyses of fabricated compound parabolic solar collector with evacuated tubes at different operating conditions: Indore (India). J Inst Eng (India): Series C 100(3):455–460. https://doi.org/10.1007/s40032-018-0455-5

Hazami M, Kooli S, Naili N, Farhat A (2013) Long-term performances prediction of an evacuated tube solar water heating system used for single-family households under typical Nord-African climate (Tunisia). Sol Energy 94:283–298. https://doi.org/10.1016/j.solener.2013.05.020

Jiang L, Widyolar B, Winston R (2015) Characterization of novel mid-temperature CPC solar thermal collectors. Energy Procedia 70:65–70. https://doi.org/10.1016/j.egypro.2015.02.098

Kabeel AE, Abdelgaied M, Elrefay MKM (2020) Thermal performance improvement of the modified evacuated U-tube solar collector using hybrid storage materials and low-cost concentrators. J Energy Storage 29:101394. https://doi.org/10.1016/j.est.2020.101394

Kerme ED, Chafidz A, Agboola OP, Orfi J, Fakeeha AH, Al-Fatesh AS (2017) Energetic and exergetic analysis of solar-powered lithium bromide-water absorption cooling system. J Clean Prod 151:60–73. https://doi.org/10.1016/j.jclepro.2017.03.060

Kerosene Prices around the world (2022) https://www.globalpetrolprices.com/kerosene_prices/#:~:text=Kerosene%20prices%2C%2028-Feb-,0.92%20U.S.%20Dollar%20per%20litre. Accessed 5 Mar 2022

LPG Prices around the world (2022) https://www.globalpetrolprices.com/lpg_prices/. Accessed 5 Mar 2022

Ma L, Lu Z, Zhang J, Liang R (2010) Thermal performance analysis of the glass evacuated tube solar collector with U-tube. Build Environ 45(9):1959–1967. https://doi.org/10.1016/j.buildenv.2010.01.015

Meyer L, Tsatsaronis G, Buchgeister J, Schebek L (2009) Exergoenvironmental analysis for evaluation of the environmental impact of energy conversion systems. Energy 34:75–89. https://doi.org/10.1016/j.energy.2008.07.018

Mills DR, Bassett IM, Derrick GH (1986) Relative cost-effectiveness of CPC reflector designs suitable for evacuated absorber tube solar collectors. Sol Energy 36(3):199–206. https://doi.org/10.1016/0038-092X(86)90135-0

Mishra RK, Garg V, Tiwari GN (2015) Thermal modeling and development of characteristic equations of evacuated tubular collector (ETC). Sol Energy 116:165–176. https://doi.org/10.1016/j.solener.2015.04.003

Mishra RK, Garg V, Tiwari GN (2017) Energy matrices of U-shaped evacuated tubular collector (ETC) integrated with compound parabolic concentrator (CPC). Sol Energy 153:531–539. https://doi.org/10.1016/j.solener.2017.06.004

Moran MJ, Shapiro HN (1993) Fundamentals of engineering thermodynamics, second edition. Eur J Eng Educ 18(2):215. https://doi.org/10.1080/03043799308928176

Panahi HKS, Dehhaghi M, Kinder JE, Ezeji TC (2019) A review on green liquid fuels for the transportation sector: a prospect of microbial solutions to climate change. Biofuel Res J 6(3):995–1024. https://doi.org/10.18331/BRJ2019.6.3.2

Pei G, Li G, Zhou X, Ji J, Su Y (2012) Comparative experimental analysis of the thermal performance of evacuated tube solar water heater systems with and without a mini-compound parabolic concentrating (CPC) reflector(C < 1). Energies 5(4):911–924. https://doi.org/10.3390/en5040911

Petela R (2003) Exergy of undiluted thermal radiation. Sol Energy 74(6):469–488. https://doi.org/10.1016/S0038-092X(03)00226-3

Petela R (2005) Exergy analysis of the solar cylindrical-parabolic cooker. Sol Energy 79(3):221–233. https://doi.org/10.1016/j.solener.2004.12.001

Rosen MA (2018) Environmental sustainability tools in the biofuel industry. Biofuel Res J 5(1):751–752. https://doi.org/10.18331/BRJ2018.5.1.2

Rosen MA, Dincer I (1997) Sectoral energy and exergy modeling of Turkey. J Energy Resource Technol Trans ASME 119(3):200–204. https://doi.org/10.1115/1.2794990

Saidur R, Ahamed JU, Masjuki HH (2010) Energy, exergy and economic analysis of industrial boilers. Energy Policy 38(5):2188–2197. https://doi.org/10.1016/j.enpol.2009.11.087

Sokhansefat T, Kasaeian A, Rahmani K, Heidari AH, Aghakhani F, Mahian O (2018) Thermoeconomic and environmental analysis of solar flat plate and evacuated tube collectors in cold climatic conditions. Renew Energy 115:501–508. https://doi.org/10.1016/j.renene.2017.08.057

Team AC (2019) CDP India Annual Report 2019: India Ranks 5th in Carbon Disclosure Project 2019, US Tops. https://affairscloud.com/cdp-india-annual-report-2019-india-ranks-5th-in-carbon-disclosure-project-2019us-tops/. Accessed 5 Mar 2022

Tsatsaronis G, Morosuk T (2012) Understanding and improving energy conversion systems with the aid of exergy-based methods. Int J Exergy 11(4):518–542. https://doi.org/10.1504/IJEX.2012.050261

Zielińska A, Skowron M, Bień A (2018) Modelling of photovoltaic cells in variable conditions of temperature and intensity of solar insolation as a method of mapping the operation of the installation in real conditions. In: 2018 International Interdisciplinary PhD Workshop (IIPhDW). IEEE, Poland. https://doi.org/10.1109/IIPHDW.2018.8388357